

Radiochemical Studies of the Transactinide Element, Rutherfordium (Rf) at JAERI

Y. Nagame*

Advanced Science Research Center, Japan Atomic Energy Research Institute, Tokai, Ibaraki 319-1195, Japan

Received: June 30, 2005; In Final Form: August 27, 2005

Radiochemical studies of element 104, rutherfordium (Rf), at JAERI (Japan Atomic Energy Research Institute) are reviewed. The transactinide nuclide ^{261}Rf has been successfully produced in the reaction $^{248}\text{Cm}(^{18}\text{O}, 5n)$ at the JAERI tandem accelerator. The excitation function of the reaction has been measured with a rotating wheel catcher apparatus and the maximum production cross section has been determined to be about 13 nb. On-line ion-exchange experiments on Rf together with the group-4 elements Zr and Hf in acidic solutions have been conducted with a rapid ion-exchange separation apparatus. From the systematic study of the anion-exchange behavior of Rf, it has been found that the properties of Rf in HCl and HNO_3 solutions are quite similar to those of Zr and Hf, definitely confirming that Rf is a member of the group-4 elements. However, we have observed an unexpected chemical behavior of Rf in HF solutions; the fluoride complex formation of Rf is significantly different from those of Zr and Hf. The current progress in the Rf aqueous chemistry is briefly summarized and prospects of extending chemical studies of transactinide elements at JAERI are considered.

1. Introduction

Presently, we know more than 20 man-made transuranium elements. According to the actinide concept,¹ the $5f$ electron series ends with element 103, lawrencium (Lr), and a new $6d$ electron transition series is predicted to begin with element 104, rutherfordium (Rf). The elements with atomic numbers $Z \geq 104$ are called transactinide elements or recently called superheavy elements.² The currently known transactinide elements, elements 104 through 112, are placed in the periodic table under their lighter homologues in the $5d$ electron series, Hf to Hg. Elements from 113 to 118 except for 117 that have been recently synthesized³⁻⁵ would be in the successive $7p$ electron series (see Figure 1), although the discoveries of elements with $Z \geq 112$ are waiting to be confirmed.⁶

Studies on the chemical properties of the elements at the uppermost end of the periodic table are extremely interesting and challenging subjects in the fields of nuclear and radiochemistry. It is also of special interest to assess the magnitude of the influence of relativistic effects on chemical properties. From the calculations of electron configurations of heavier elements, it is predicted that sudden changes in the structure of electron shells may appear due to relativistic effects which originate from the increasingly strong Coulomb field of a highly charged atomic nucleus.⁷ Therefore, it is expected that heavier elements show a drastic rearrangement of electrons in their atomic ground states, and as electron configurations are responsible for chemical behavior of elements, such relativistic effects can lead to surprising chemical properties. Increasing deviations from the periodicity of chemical properties based on extrapolation from lighter homologues in the periodic table are consequently predicted.^{2, 8-10} It would be no longer possible to deduce detailed chemical properties of the transactinide elements simply from the position in the periodic table.

The transactinide elements must be produced at accelerators using reactions of heavy-ion beams with heavy target materials and must be identified by measurement of their decay or that of their known daughter nuclei with unambiguous detection techniques. Chemical experiments with the transactinide

1																	18
H																	He
3	4											13	14	15	16	17	18
Li	Be											B	C	N	O	F	Ne
11	12											13	14	15	16	17	18
Na	Mg	3	4	5	6	7	8	9	10	11	12	Al	Si	P	S	Cl	Ar
19	20	21	22	23	24	25	26	27	28	29	30	31	32	33	34	35	36
K	Ca	Sc	Ti	V	Cr	Mn	Fe	Co	Ni	Cu	Zn	Ga	Ge	As	Se	Br	Kr
37	38	39	40	41	42	43	44	45	46	47	48	49	50	51	52	53	54
Rb	Sr	Y	Zr	Nb	Mo	Tc	Ru	Rh	Pd	Ag	Cd	In	Sn	Sb	Te	I	Xe
55	56	57	72	73	74	75	76	77	78	79	80	81	82	83	84	85	86
Cs	Ba	La	Hf	Ta	W	Re	Os	Ir	Pt	Au	Hg	Tl	Pb	Bi	Po	At	Rn
87	88	89	104	105	106	107	108	109	110	111	112	113	114	115	116	117	118
Fr	Ra	Ac	Rf	Db	Sg	Bh	Hs	Mt	Ds	Rg	112	113	114	115	116	117	118
Lanthanides		57	58	59	60	61	62	63	64	65	66	67	68	69	70	71	
Actinides		89	90	91	92	93	94	95	96	97	98	99	100	101	102	103	
		Ac	Th	Pa	U	Np	Pu	Am	Cm	Bk	Cf	Es	Fm	Md	No	Lr	

Figure 1. Periodic table of the elements.

elements are generally divided into the following 4 basic steps: i) synthesis of transactinide nuclides, ii) rapid transport of the synthesized nuclides to chemical separation apparatuses, iii) fast chemical isolation of a desired nuclide and preparation of a sample suitable for nuclear spectroscopy, and iv) detection of nuclides through their characteristic decay properties. Because of the short half-lives and the low production rates of the transactinide nuclides, each atom produced decays before a new atom is synthesized. This means that any chemistry to be performed must be done on an "atom-at-a-time" basis. Thus, rapid and very efficient radiochemical procedures must be devised. Recent comprehensive reviews on the chemistry of the transactinide elements are seen in References 2, 11, and 12.

In order to carry out chemical experiments of the transactinide elements with single atoms, we developed some experimental apparatuses: a beam-line safety system for the usage of a gas-jet coupled with a radioactive target and recoil chamber, a rotating wheel catcher apparatus for the measurement of α and spontaneous fission (SF) decay of transactinide nuclei, and an automated rapid ion-exchange separation apparatus based on high performance liquid chromatography coupled with an on-line α -particle detection system.¹³

The transactinide nuclide, 78-s ^{261}Rf , that is commonly used for recent chemical studies of element 104, was successfully produced in the reaction $^{248}\text{Cm}(^{18}\text{O}, 5n)$ at the JAERI tandem accelerator for the first time in Japan. The excitation function of the reaction was measured with the rotating wheel catcher apparatus MANON (Measurement system for Alpha particle and spontaneous fission ON-line), and the maximum

*Corresponding author. E-mail: nagame.yuichiro@jaea.go.jp. FAX: +81-29-282-5927.

production cross section was determined to be 13 nb at around 94-MeV ^{18}O energy.¹⁴ On-line anion-exchange experiments of Rf together with the group-4 elements Zr and Hf in acidic solutions, HCl, HNO_3 , and HF, were conducted with the rapid ion-exchange separation apparatus, AIDA (Automated Ion-exchange separation apparatus coupled with the Detection system for Alpha-spectroscopy).^{15, 16} AIDA enables us to perform cyclic discontinuous column chromatographic separations of short-lived nuclides in aqueous solutions and automated detection of α -particles within a typical cycle of 1–2 min. The adsorption behavior of Rf as a function of the acid concentration has been systematically studied with AIDA.^{15, 16}

In this paper, the progress in the radiochemical studies of Rf and future research plans for extending chemical studies of the transactinide elements at JAERI are summarized.

2. Production of the Transactinide Nuclide ^{261}Rf

A schematic representation of the experimental set-up including a target and recoil chamber arrangement and the rotating wheel catcher apparatus MANON is shown in Figure 2. A ^{248}Cm target of 590- $\mu\text{g}/\text{cm}^2$ thickness prepared by electrodeposition of $\text{Cm}(\text{NO}_3)_3$ from isopropyl alcohol onto a 2.2- mg/cm^2 -thick beryllium backing foil was bombarded by an ^{18}O beam delivered from the JAERI tandem accelerator. The $^{18}\text{O}^{6+}$ beam passed through a 2.0- mg/cm^2 HAVAR entrance window foil, 0.09- mg/cm^2 He cooling gas and the beryllium target backing, and finally entering the ^{248}Cm target material. The beam intensity was 250–300 particle nA. The reaction products recoiling out of the target were stopped in a volume of He gas (≈ 1 bar) that had been loaded with potassium chloride (KCl) aerosols generated by sublimation from the surface of KCl powder at 640 °C. The products adsorbed onto the surface of the aerosols were swept out of the recoil chamber with the He gas flow (2.0 L/min) and were transported through a Teflon-capillary (2.0 mm i.d., 20 m long) by a He/KCl gas-jet system to MANON. The transported nuclei were deposited on polyethylene terephthalate foils of 120 $\mu\text{g}/\text{cm}^2$ thickness and 20 mm diameter mounted on the circumference of a stepwise rotating stainless steel wheel that has 80-position collection sites with an 80-cm diameter. The wheel was rotated every 110 s to position the foils between six pairs of Si PIN photodiodes for α -particle detection. Each detector had an active area of $18 \times 18 \text{ mm}^2$. A detection efficiency of approximately 40% for α -particles was achieved. The energy resolution (FWHM) was about 30 keV for the top detectors and was 100 keV for the bottom ones.

To determine the gas-jet transport yield, we first collected the recoil of ^{252}Md ($T_{1/2} = 2.3$ min) produced in the reaction

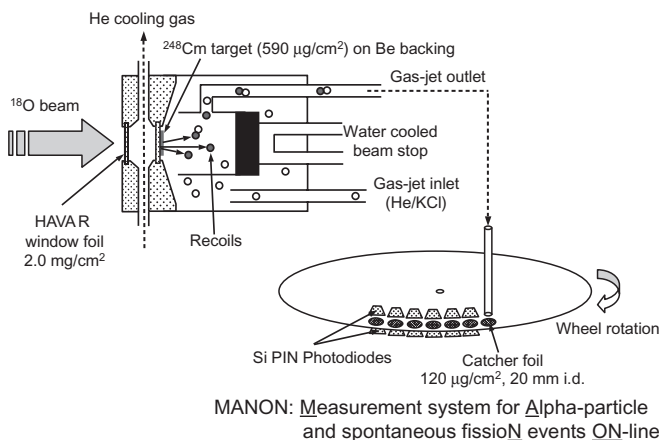


Figure 2. Schematic representation of a target and recoil chamber arrangement with a He/KCl gas-jet system and the apparatus MANON (Measurement system for Alpha-particle and spontaneous fission events ON-line).

$^{238}\text{U}(^{19}\text{F}, 5n)$ behind the target in an aluminum catcher foil to get a reference value (100%), while ^{252}Md transported by the gas-jet was collected on a glass filter. ^{252}Fm ($T_{1/2} = 25$ h), the EC decay daughter of ^{252}Md , in both samples was chemically separated and subjected to α -spectroscopy. By comparing the production rate measured after transport through the gas-jet with the absolute production rate from the catcher foil, the transport efficiency was determined to be approximately 35%. The production cross sections were evaluated from the measurement of the mother-daughter correlations of α -particle energies between ^{261}Rf ($E_\alpha = 8.28$ MeV) and 25-s ^{257}No ($E_\alpha = 8.22, 8.27, \text{ and } 8.32$ MeV).¹⁷ A photograph of the MANON apparatus is shown in Figure 3.

The sum of α -particle spectra measured in the six top detectors for the production of ^{261}Rf at 94-MeV ^{18}O beam energy is shown in Figure 4. The total beam dose was 2.35×10^{16} . In the α -energy range of 8.10–8.40 MeV, α lines from ^{261}Rf and its daughter ^{257}No are clearly seen. No contributions from other nuclides in this energy window are observed, although there exist several α lines originating from the transfer reaction products from the Pb impurity in the ^{248}Cm target. A total of 166 events were registered both in the top and bottom detectors in the singles measurement and 57 α - α correlation events were detected at this beam energy. Assuming a 100% α -decay branch for both ^{261}Rf and ^{257}No ,¹⁷ the production cross sections of ^{261}Rf in this reaction were evaluated to be $8 \pm 2, 13 \pm 3, \text{ and } 8 \pm 2$ nb at the ^{18}O beam energies of 91, 94, and 99 MeV, respectively. The contribution of the direct production of ^{257}No via the $^{248}\text{Cm}(^{18}\text{O}, \alpha 5n)$ reaction is assumed to be negligible in the studied energy region. In Figure 5, the cross sections are plotted as a function of the ^{18}O bombarding energy together with the literature data,^{18, 19} where the relative cross section values in Reference 19 are normalized to the present results. The maximum cross section of about 13 nb at the ^{18}O energy of 94 MeV was obtained.¹⁴ This results in a production rate of about 2 atoms per min under the given conditions.

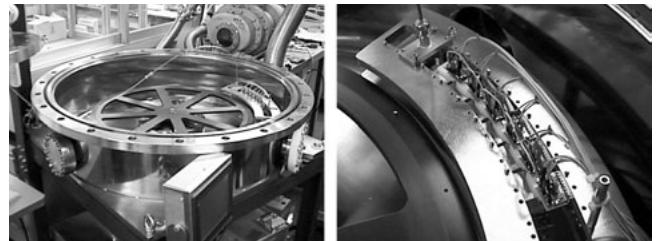


Figure 3. View of the MANON (left) and the part of the detectors inside the apparatus (right).

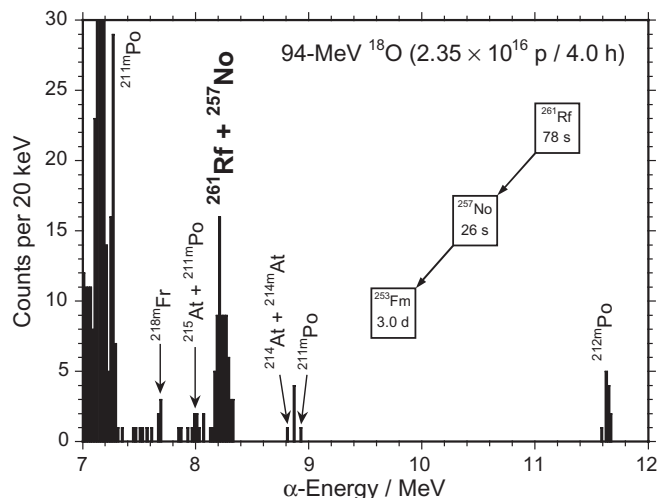


Figure 4. Sum of α -particle spectra measured in the bombardment of the ^{248}Cm target with 94-MeV ^{18}O ions.

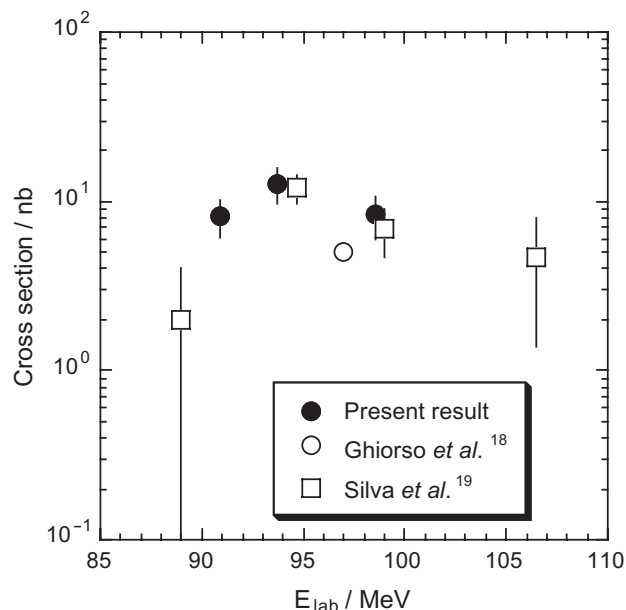


Figure 5. Excitation function for the $^{248}\text{Cm}(^{18}\text{O}, 5n)$ reaction. The data taken from References 18 and 19 are also shown.

3. Aqueous Chemistry of Element 104 Rf

The pioneering works, the first generation experiments, so far performed have concentrated on the question how well the periodic table accommodates the transactinide elements as transition metals in the seventh period. The results with a few atoms have justified placing the elements Rf through element 108, hassium (Hs), into groups 4 to 8 of the periodic table.² However, the first generation experiments still show conflicting results and some of them are criticized due to unsatisfactory experimental conditions.²⁰ There are few convincing data for examining relativistic effects and for considering thermodynamic chemical properties of the transactinide elements even in those of Rf and element 105, dubnium (Db). Therefore, it is of great importance to study detailed chemical properties of the transactinide elements with high statistics and to compare these with properties deduced from extrapolations of periodicity and from modern relativistic molecular orbital calculations: the second generation experiments. In the following, the second generation studies on Rf at JAERI are outlined.

3.1. On-line Production of ^{261}Rf , ^{169}Hf , and ^{85}Zr . As mentioned above, one of our experimental approaches is a detailed comparison of the chemical properties of Rf with those of the expected lighter homologues Hf and Zr. Thus, the chemical experiments on Rf should be conducted together with the homologues under strictly identical conditions. For the on-line production of Rf and the homologues, we used two different targets; one was the mixed target of ^{248}Cm (610 $\mu\text{g}/\text{cm}^2$ in thickness) and Gd (39.3%-enriched ^{152}Gd of 36 $\mu\text{g}/\text{cm}^2$ in thickness) prepared by electrodeposition onto a 2.4-mg/ cm^2 beryllium foil for the simultaneous production of ^{261}Rf and 3.24-min ^{169}Hf via the $^{248}\text{Cm}(^{18}\text{O}, 5n)$ and $\text{Gd}(^{18}\text{O}, xn)$ reactions, respectively. The other was the ^{nat}Gd (370- $\mu\text{g}/\text{cm}^2$ thickness) and ^{nat}Ge (660- $\mu\text{g}/\text{cm}^2$ thickness) mixed target to produce ^{169}Hf and 7.86-min ^{85}Zr through the $^{nat}\text{Gd}(^{18}\text{O}, xn)$ and $^{nat}\text{Ge}(^{18}\text{O}, xn)$ reactions, respectively. The ^{nat}Gd was electrodeposited on a 2.7-mg/ cm^2 beryllium backing and then, on the resulting ^{nat}Gd target, ^{nat}Ge was deposited by vacuum evaporation.^{15, 16} The reaction products recoiling out of the target were transported through a Teflon-capillary to the chemistry laboratory by the He/KCl gas-jet system as described in Section 2.

3.2. Atom-at-a-time Chemistry of Rf. The chemical study needs to be carried out on phenomena that give the same results for only a few atoms and for macro amounts of atoms; the question arises as to whether a meaningful chemistry with

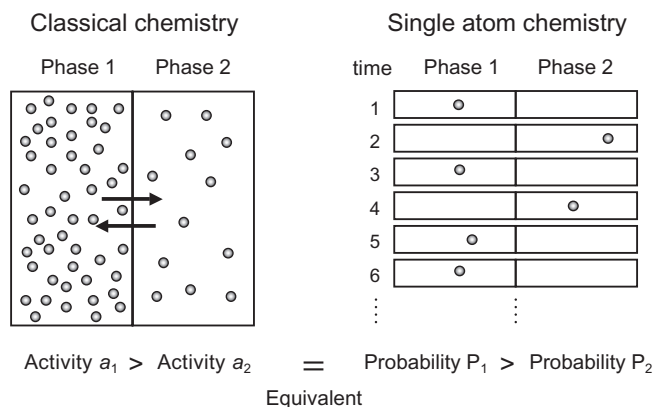


Figure 6. Concept for single atom chemistry. Courtesy of M. Schädel.

single atoms is possible. For single atoms, the classical law of mass action is no longer valid, because the atom cannot exist in the different chemical forms taking part in the chemical equilibrium at the same time. Guillaumont et al. suggested for single-atom chemistry the introduction of a specific thermodynamic function, the single-particle free enthalpy.^{21, 22} An expression equivalent to the law of mass action is derived, in which activities are replaced by probabilities of finding the species in the appropriate phases. According to this law, an equilibrium constant (distribution coefficient) of the atom between two phases is correctly defined in terms of the probabilities of finding the atom in one phase or the other. If a static partition method is used, this coefficient must be measured in repetitive experiments. Since dynamical partition methods can be considered as repetitive static partitions, the displacement of the atom along the chromatographic column gives a statistical result.^{2, 11} The concept for single atom chemistry is depicted in Figure 6.

For short-lived atoms, the partition equilibrium must be reached during the lifetime of the nuclides, which requires fast reaction kinetics. Based on the kinetics of a single-step exchange reaction, Borg and Dienes suggested that at certain conditions a measurement of the partition of the atom between the phases with very few atoms will already yield an equilibrium constant close to the "true" value provided that both states are rapidly sampled.²³ The above interpretation indicates that chromatographic systems with fast kinetics are ideally suited for single atom separation as there is rapid, multiple sampling of the adsorbed or mobile chemical species.^{2, 11}

To perform rapid and repetitive chemical experiments with Rf, we employed the apparatus AIDA^{15, 24} that consists of a modified ARCA (Automated Rapid Chemistry Apparatus)²⁵ which is a miniaturized computer controlled liquid chromatography system, and an automated on-line α -particle detection system. The schematic drawing of AIDA is given in Figure 7. There are two column magazines, each containing 20 microcolumns. In the modified ARCA as shown in Figure 8, two different paths to supply solutions are available; the first eluent goes through the collection site to the microcolumn, while the second is directed to the column after one-step forward movement of the column magazine to avoid cross-contamination at the collection site.

3.3. Anion-exchange Behavior of Rf in HCl and HNO₃. The experimental procedures and the result on the anion-exchange behavior of Rf in HCl solution are summarized here. The reaction products recoiling from the target were transported by the He/KCl gas-jet system to the collection site of AIDA (see Figure 8). After collection for 125 s, the site was mechanically moved to the top of one of the microcolumns, where the products were dissolved with 170 μL of hot ($\approx 80^\circ\text{C}$) 11.5 M HCl and were fed onto the 1.6 mm i.d. \times 7.0 mm chromatographic column filled with the anion-exchange resin

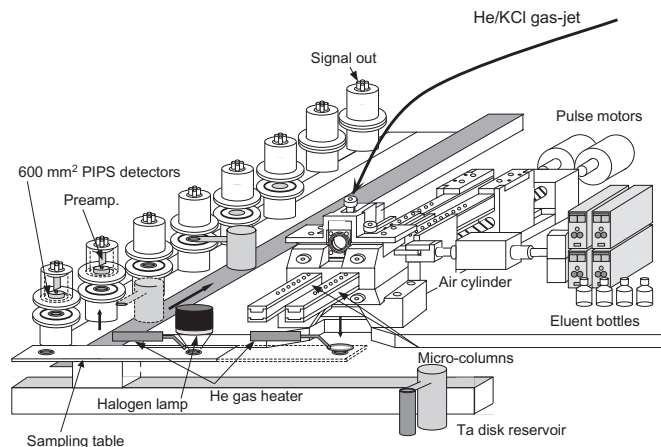


Figure 7. Schematic drawing of AIDA (Automated Ion-exchange separation apparatus) coupled with the Detection system for Alpha spectroscopy).

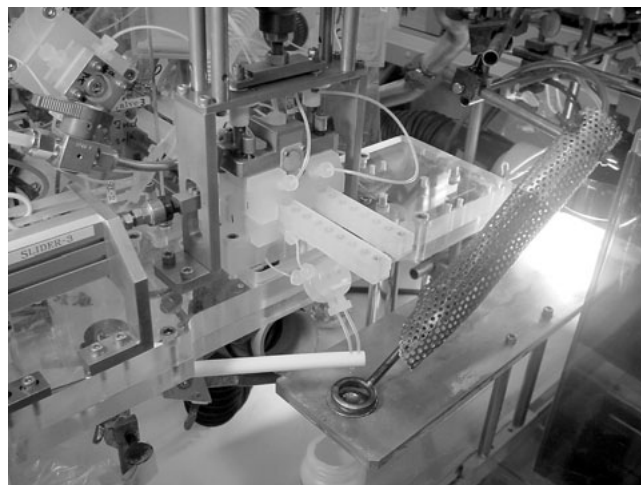


Figure 9. Photograph of the sample collection part of AIDA.

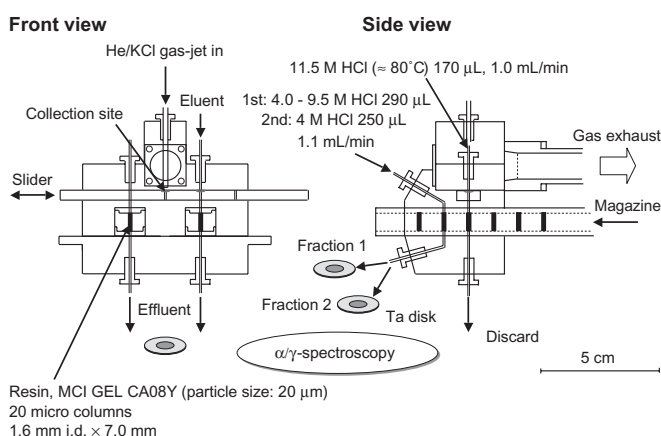


Figure 8. Schematic of the modified ARCA in AIDA.

MCI GEL CA08Y (particle size of about 20 μm) at a flow rate of 1.0 mL/min. Then, the products were eluted with 290 μL of HCl through the second path with concentrations between 4.0 M and 9.5 M at a flow rate of 1.1 mL/min. The effluent was collected on a Ta disk as fraction 1 and evaporated to dryness using hot He gas and a halogen heat lamp for α -particle measurement (see Figure 7). The remaining products in the column were eluted with 250 μL of 4.0 M HCl at a flow rate of 1.1 mL/min. The effluent was collected on another Ta disk and evaporated to dryness as fraction 2. The pair of disks were automatically transported to the α -spectroscopy station equipped with eight 600- mm^2 PIPS (passivated ion-implanted planar silicon) detectors. Counting efficiencies of each detector ranged from 30% to 40% depending on geometric differences of the dried α sources. Alpha-particle energy resolution was 80–200 keV FWHM.^{15, 16} After the α -particle measurement, the 493 keV γ -radiation of ^{169}Hf was monitored with Ge detectors to determine the elution behavior of Hf and its chemical yield. The anion-exchange experiments with ^{85}Zr and ^{169}Hf produced from the Ge/Gd mixed target were conducted under the same conditions as those with ^{261}Rf and ^{169}Hf . The effluents were collected in polyethylene tubes and were assayed by γ -ray spectroscopy.¹⁵ Each separation was accomplished within 20 s and the α -particle measurement was started within 80 s after the collection of the products at the AIDA collection site. The chemical yield of ^{169}Hf including deposition and dissolution efficiencies of the aerosols was approximately 60%.¹⁵ A photograph of the effluent collection part of AIDA is shown in Figure 9.

Figures 10(a) and 10(b) show the typical α spectra observed in the elution with 11.5 M HCl and with 4.0 M HCl, respectively.²⁶ There are only a few α events from the α decay of ^{261}Rf – ^{257}No

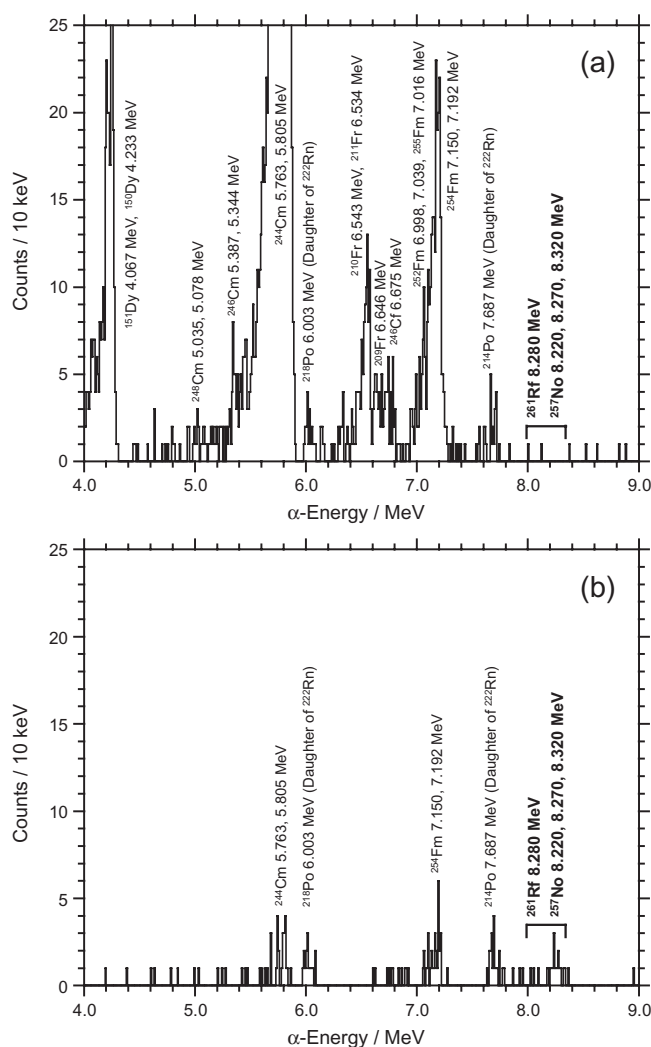


Figure 10. α -particle spectra of samples prepared from the elution fractions: (a) 11.5 M HCl and (b) 4.0 M HCl. Data taken from Reference 26.

at 11.5 M HCl, which means Rf is strongly adsorbed on the anion-exchange resin, while at 4.0 M HCl, Rf is not retained in the column.

In order to evaluate the contribution to the adsorption distribution of ^{261}Rf on the anion-exchange resin of the α events from ^{257}No formed from the α decay of ^{261}Rf during the collection at AIDA before the chemical separation, the adsorption behavior of No on the same anion-exchange resin was examined. On-line experiments with ^{255}No produced in the reaction $^{248}\text{Cm}(^{12}\text{C}, 5n)$ were separately conducted according to those with ^{261}Rf in HCl

and HNO₃ solutions,²⁷ and it was found that this contribution was negligible.²⁷ As shown in Figure 10(a), the Cm isotopes, recoil products of the target, the isotopic composition of the ²⁴⁸Cm target is as follows: ²⁴⁴Cm (1.12 at.%) and ²⁴⁶Cm (1.31 at.%), and the Fm isotopes, transfer reaction products from the Cm target, are mostly eluted with 11.5 M HCl. The present result is consistent with the fact that the chloride complex formation of element 104 in 12 M HCl was stronger than that of the trivalent actinides as reported by Hulet et al.²⁸ The trivalent rare earth element isotopes in the figure, ^{150,151}Dy, the transfer reaction products from the ¹⁵²Gd target, are also eluted with 11.5 M HCl.

From the 1893 cycles of the anion-exchange experiments, a total of 186 α events from ²⁶¹Rf and its daughter ²⁵⁷No were registered including 35 α - α correlation events.¹⁵ Figure 11(a) shows the adsorption behavior of Rf, Zr, and Hf as a function of HCl concentration. The ordinate shows the adsorption probabilities of these elements, %ads = 100A₂/(A₁ + A₂), where A₁ and A₂ are the eluted radioactivities observed in fractions 1 and 2, respectively. It should be noted here that the data of Hf from both targets are in very good agreement. The adsorption behavior of Rf is quite similar to those of the group-4 elements Zr and Hf. The adsorption of these elements rapidly increases with increasing HCl concentration above 7 M: typical anion-exchange behavior of the group-4 elements. This means that anionic chloride complexes of the tetravalent Rf, Zr, and Hf are formed above 7 M HCl. On the other hand, the adsorption of the tetravalent pseudo-homologue thorium (Th) in HCl concentrations above 8 M is quite different from that of Rf, Zr, and Hf as shown in Figure 11(b); Th does not form anionic complexes in this region of concentration. The distribution coefficients (*K_d*) for Zr, Hf, and Th in Figure 11(b) were obtained by the batch method using radiotracers of ⁸⁸Zr, ¹⁷⁵Hf,

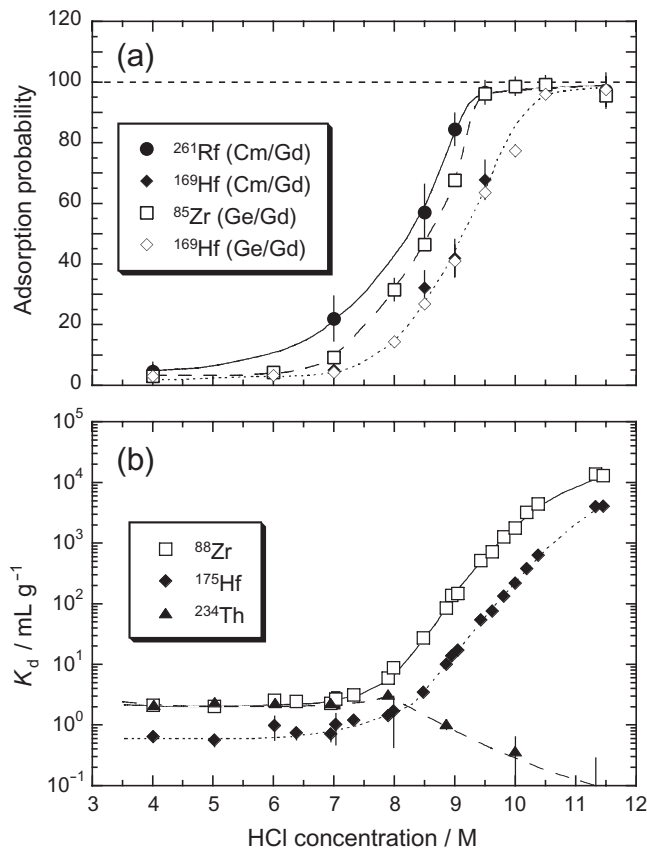


Figure 11. (a) Adsorption probability (%ads) of Rf, Zr, and Hf on the anion-exchange resin CA08Y as a function of HCl concentration. The data for ²⁶¹Rf and ¹⁶⁹Hf obtained from the Cm/Gd target are shown by closed symbols, while those for ⁸⁵Zr and ¹⁶⁹Hf from the Ge/Gd target are by open symbols. (b) Distribution coefficients (*K_d*) for Zr, Hf, and Th on the anion-exchange resin CA08Y as a function of HCl concentration. Data taken from Reference 15.

and ²³⁴Th, respectively.¹⁵ Another interesting feature is the adsorption sequence on the anion-exchange resin among Rf, Zr, and Hf. The adsorption order that reflects the strength of the chloride complex formation is Rf \geq Zr > Hf. The present outcome, however, contradicts the prediction with the relativistic molecular density-functional calculations by Pershina et al. where the sequence of the chloride complex formation is expected to be Zr > Hf > Rf.²⁹

In order to obtain information on the chemical species and structure of Rf complexes in HCl, we performed measurements of the extended X-ray absorption fine structure (EXAFS) spectra of Zr and Hf chloride complexes at the KEK (High Energy Accelerator Research Organization) Photon Factory.^{30,31} It has been found that the Zr and Hf complex structure in HCl solution changes from presumably [M(H₂O)₈]⁴⁺ (M = Zr and Hf) to the anionic chloride complex [MCl₆]²⁻ with the increase in the HCl concentration from 9 to 12 M, which is consistent with the results of the anion-exchange experiments. Therefore, we assume the structure of the Rf complex, in analogy to those of Zr and Hf, is the octahedral [RfCl₆]²⁻ in conc. HCl. The difference in the strength of the chloride complex formation of Zr and Hf was also demonstrated; the affinity of the Cl⁻ ion for Zr is higher than that for Hf: [ZrCl₆]²⁻ > [HfCl₆]²⁻,³¹ which agrees with the adsorption sequence in Figures 11(a) and 11(b) and the result by Huffman et al.³² This confirms that the sequence in the chloride complex strength among these elements is Rf \geq Zr > Hf.

Non Th⁴⁺-like behavior of Rf was also probed with anion-exchange experiments in 8 M HNO₃. From 217 experiments, a total of 20 α events from ²⁶¹Rf and ²⁵⁷No were observed including 5 time-correlated α pairs. Although Th⁴⁺ formed anionic complexes and was strongly adsorbed on the anion-exchange resin, Rf was eluted from the column with 8 M HNO₃ as expected for a typical group-4 element as shown in Figure 12.¹⁵ The adsorption value for Th was obtained by batch experiments using radiotracer ²³⁴Th.¹⁵ The above results definitely confirm that Rf is a member of the group-4 elements, but does not resemble the pseudo-homologue Th.

3.4. Fluoride Complex Formation of Rf. The experimental procedures with AIDA are basically the same as those described in Section 3.3 and the details are given in Reference

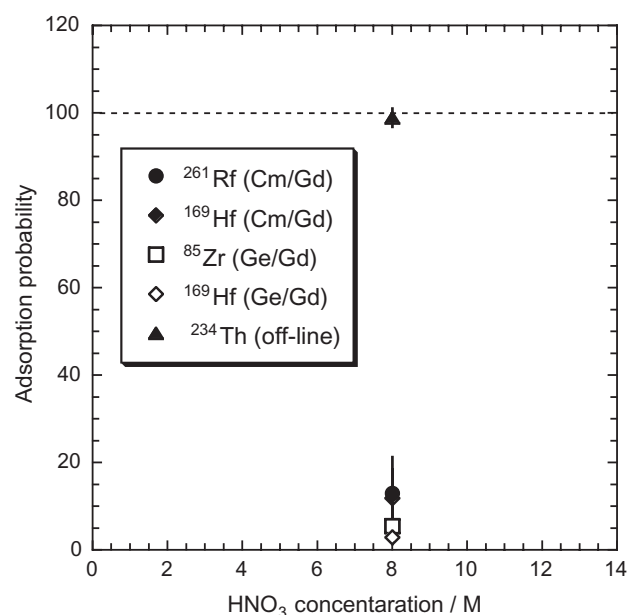


Figure 12. Adsorption probability (%ads) of Rf, Zr, and Hf on the anion-exchange resin CA08Y at 8 M HNO₃ concentration. The data for ²⁶¹Rf and ¹⁶⁹Hf obtained from the Cm/Gd target are shown by closed symbols, while those for ⁸⁵Zr and ¹⁶⁹Hf from the Ge/Gd target are by open symbols. The adsorption of Th (closed triangle) was obtained by the separate off-line experiment. Data taken from Reference 15.

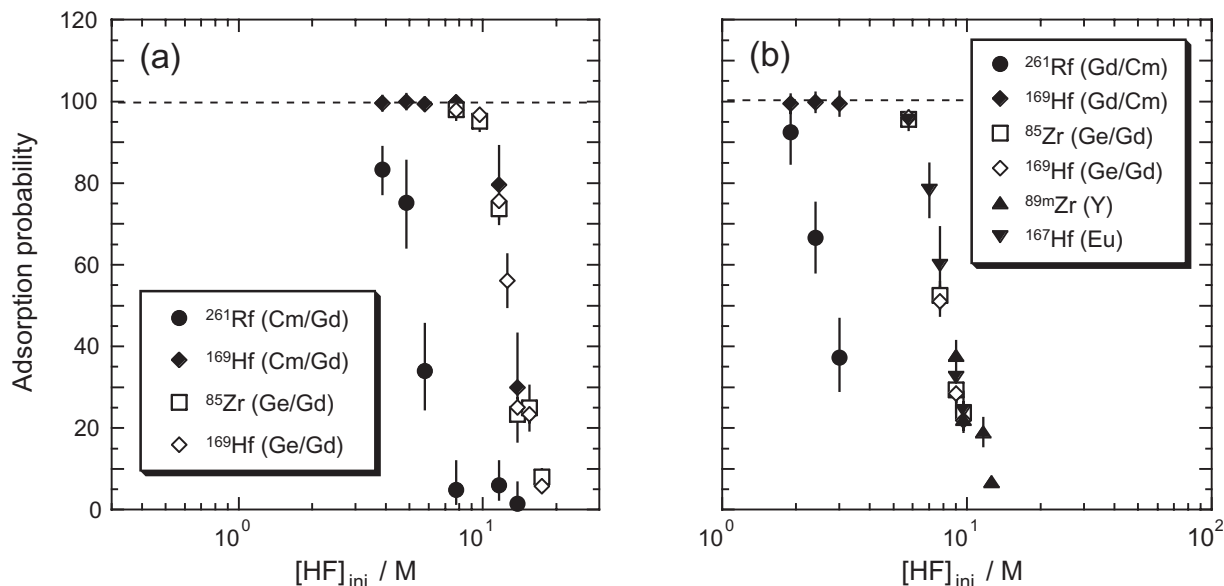


Figure 13. Adsorption behavior of Rf, Zr, and Hf on the anion-exchange resin CA08Y as a function of the initial concentration of HF, $[HF]_{ini}$ obtained with (a) the 1.6 mm i.d. \times 7.0 mm column and with (b) the 1.0 mm i.d. \times 3.5 mm one. The data for ^{261}Rf and ^{169}Hf obtained from the Cm/Gd target are shown by closed symbols, while those for ^{85}Zr and ^{169}Hf from the Ge/Gd target are by open ones. The adsorption values of ^{89m}Zr and ^{167}Hf produced from the ^{89}Y and ^{nat}Eu targets, respectively, are also included in (b). Data taken from Reference 16.

16. In this study, we used two different microcolumns, 1.6 mm i.d. \times 7.0 mm and 1.0 mm i.d. \times 3.5 mm, to measure a wide range of K_d values. From the 4226 cycles of the anion-exchange experiments, a total of 266 α events from ^{261}Rf and its daughter ^{257}No were registered including 25 time-correlated α pairs of ^{261}Rf and ^{257}No . Figures 13(a) and 13(b) show the variation of the adsorption probability of Rf, Zr, and Hf as a function of the initial concentration of HF, $[HF]_{ini}$ for the two columns.¹⁶ The adsorption values of Zr and Hf were also measured in separate experiments using ^{89m}Zr and ^{167}Hf produced in the $^{89}\text{Y}(p, n)$ and $^{nat}\text{Eu}(^{19}\text{F}, xn)$ reactions, respectively.¹⁶ The contribution of the α events from the daughter nucleus ^{257}No formed from the α decay of ^{261}Rf before the chemical separation procedures was also evaluated to be less than 5% in HF solution.³³ As shown in Figure 13, the adsorption values of Zr and Hf obtained in the different experiments agree well, and the adsorption of Zr and Hf is absolutely equal over a wide range of HF concentrations and steeply decreases with $[HF]_{ini}$, while that of Rf decreases at much lower $[HF]_{ini}$. The lower adsorption of Rf indicates that the fluoride complex formation of Rf is weaker than those of Zr and Hf. The present result is consistent with those reported in References 34–37 where a different behavior of Rf as compared to that of the homologues in the fluoride complex formation was observed.

It is well known that the dissociation of HF is as follows,³⁸



According to the dissociation constants $K_1 = 935 \text{ M}^{-1}$ and $K_2 = 3.12 \text{ M}^{-1}$ for eqs (1) and (2), respectively,³⁸ above 1 M $[HF]_{ini}$, the concentration of the anionic HF_2^- species is more than one order of magnitude higher than that of the free F^- . Thus, the K_d values for Rf, Zr, and Hf in Figure 14 are plotted as a function of the concentration of HF_2^- , $[\text{HF}_2^-]$.²⁴ The K_d values for Rf were deduced from the adsorption probability in Figure 13 by assuming that the kinetics in the fluoride complex formation and the anion-exchange processes of Rf are as fast as those of the homologues Zr and Hf as described in Reference 16, while those for Zr and Hf were from the on-line column chromatographic experiments with AIDA. A decrease of the K_d values for these elements with $[\text{HF}_2^-]$ is explained as the displacement

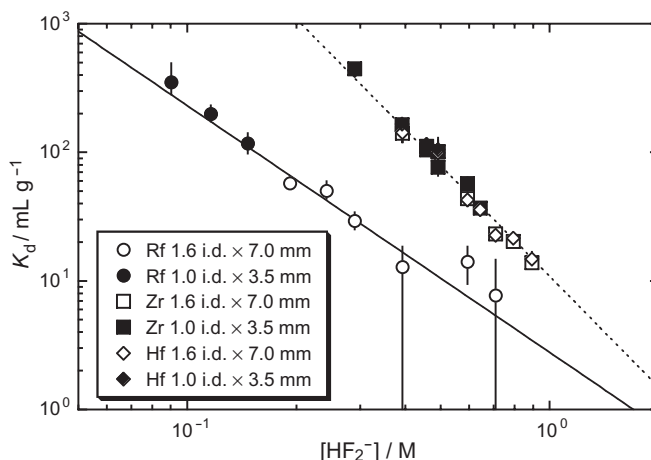
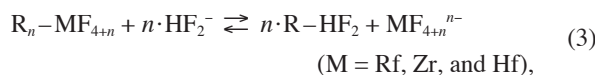


Figure 14. Distribution coefficients (K_d) for Rf, Zr, and Hf on the anion-exchange resin CA08Y as a function of the concentration of HF_2^- . The data from the 1.6 mm i.d. \times 7.0 mm and 1.0 mm i.d. \times 3.5 mm columns are depicted by open and closed symbols, respectively. Data taken from References 16 and 24.

of the metal complex from the binding sites of the resin by the counter anion HF_2^- as,



where R denotes the resin. As shown in Figure 14, the K_d values of these elements decrease linearly with $[\text{HF}_2^-]$ in the $\log K_d$ vs. $\log [\text{HF}_2^-]$ plot. It should be noted that the slopes for Zr and Hf are clearly -3 (dashed line), while that for Rf is significantly different, i.e. -2 (solid line). Equation 3 implies then that Rf is likely to be present as the hexafluoro complex, $[\text{RfF}_6]^{2-}$ similar to the well known $[\text{ZrF}_6]^{2-}$ and $[\text{HfF}_6]^{2-}$ at lower $[HF]_{ini}$, while Zr and Hf are likely to be present in the form of the heptafluoro complexes, $[\text{ZrF}_7]^{3-}$ and $[\text{HfF}_7]^{3-}$ as suggested in References 39 and 40. The activity coefficients of the involved chemical species, however, are not available in the case of the higher concentration of HF, thus the definite identification of the anionic fluoride complexes is presently an open question.

Recently, we have studied the anion-exchange behavior of Rf in the mixed HF/ HNO_3 solutions to further the understanding of

the fluoride complex formation of Rf. The K_d values for Rf and the homologues Zr and Hf have been measured as a function of the fluoride ion concentration $[F^-]$.⁴¹ The results indicate that at constant concentration of the nitrate ion $[NO_3^-] = 0.01$ M, the formation of the hexafluoro anionic complexes of Zr and Hf occurs at a fluoride ion concentration of about 10^{-5} M, while that of Rf started at around 10^{-3} M. There was about two-orders of magnitude difference in the fluoride ion concentration of Rf and the homologues for the formation of the hexafluoro complexes. This also clearly demonstrates that the formation of the fluoride complexes of Rf is much weaker than those of the homologues Zr and Hf.⁴¹

Relativistic density-functional calculations of the electronic structures of hexafluoro complexes ($[MF_6]^{2-}$, M=Rf, Zr, and Hf) have been performed to evaluate the stability of the complexes. The results indicate that the sequence in the overlap populations between the valence d orbitals of M^{4+} and the valence orbitals of F^- is found to be $Zr \approx Hf > Rf$, suggesting that the Rf complex is less stable than those of Zr and Hf in the $[MF_6]^{2-}$ structure.⁴² Although the calculations qualitatively agree with the experimental results, further theoretical approaches are needed to quantitatively understand the present interesting results.

4. Summary and Perspectives

Anion-exchange behavior of rutherfordium ^{261}Rf produced in the $^{248}\text{Cm}(^{18}\text{O}, 5n)$ reaction was systematically studied based on an atom-at-a-time scale. The adsorption probabilities of Rf in anion-exchange chromatography were measured with high statistics, which has made it possible to perform a detailed comparison of the properties of Rf with those of the homologues Zr and Hf. It was found that the anion-exchange behavior of Rf is quite similar to those of Zr and Hf in HNO_3 and HCl solutions, clearly confirming that Rf is a member of the group-4 elements, and Rf does not behave like the tetravalent pseudo-homologue Th. On the other hand, a large difference in the adsorption behavior of Rf and the homologues on the anion-exchange resin was observed in HF solution; the fluoride complex formation of Rf is much weaker than those of the homologues. According to the HSAB (Hard and Soft Acids and Bases) concept,⁴³ the fluoride anion is a hard anion and interacts stronger with (hard) small cations. Thus, a weaker fluoride complex formation of Rf as compared to Zr and Hf would be reasonable if the size of the Rf^{4+} ion is larger than those of Zr^{4+} and Hf^{4+} (0.08 nm vs. 0.07 nm) as predicted by Johnson and Fricke.⁴⁴ The fact that the chloride complex formation of Rf is slightly stronger than those of the homologues would also be explained by this concept, because the chloride anion is a relatively soft anion. (The different adsorption behavior of Zr and Hf in HCl is not interpreted with this concept, since the radii of Zr^{4+} and Hf^{4+} are known to be very similar.) To enhance the understanding of the chemical properties of Rf, the complex formation study with the softer halide anions (Br^- and I^-) will give some valuable information. Quantitative theoretical calculations are also required to gain more knowledge on the complex chemistry of Rf.

In further studies of Rf aqueous chemistry, experiments on reversed-phase extraction chromatography with AIDA are under way to study complex formation ability of Rf with various kinds of organic extractants. Also experiments are being performed to obtain some thermodynamic equilibrium constants of Rf in fluoride complex formation. On the basis of these quantitative data, the influence of relativistic effects on chemical properties of Rf will be discussed.

Anion-exchange experiments with 34-s ^{262}Db produced in the $^{248}\text{Cm}(^{19}\text{F}, 5n)$ reaction with the cross section of 1.3 nb are also being conducted with AIDA.^{30,45} To obtain more accurate data, however, we need to develop a new device to shorten the time for the preparation of the α sources. An improved AIDA

based on a continuous ion-exchange system is under construction.

Acknowledgment. The research work reported was carried out by many colleagues that make up the Heavy Element Nuclear Chemistry Group at JAERI. The list includes K. Akiyama, M. Asai, S. Goto, H. Haba, M. Hirata, S. Ichikawa, Y. Ishii, I. Nishinaka, M. Sakama, T. K. Sato, A. Toyoshima, and K. Tsukada. The present study is supported in part by the JAERI-University Collaboration Research Program and by the Program on the Scientific Cooperation between JAERI and GSI in Research and Development in the Field of Ion Beam Application. We would like to thank all colleagues participated in the experiment and contributed to this study from Wako, Niigata, Osaka, Kanazawa, Tokyo, Tsukuba, Shizuoka, Tokushima, Darmstadt, Mainz, Bern/Villigen, and Munich. We are grateful to M. Schädel for his continuous help and valuable suggestions from the beginning of this work. We also acknowledge W. Brüchle, H. W. Gäggeler, H. Kudo, J. V. Kratz, Y. Oura, A. Shinohara, K. Sueki, A. Türler, and A. Yokoyama for their kind and constant support. Our thanks go to the staff of the JAERI tandem accelerator, Advanced Science Research Center, and Nuclear Physics Group at JAERI, and other all colleagues for their continuous help. The author appreciates kindness of P. J. Karol for reading and correcting the manuscript. Last, he is sincerely indebted to H. Nakahara for his thoughtful and constant advice and encouragement throughout the course of this work.

References

- (1) G. T. Seaborg, *Chem. Eng. News* **23**, 2190 (1945).
- (2) *The Chemistry of Superheavy Elements*, ed. M. Schädel, Kluwer Academic Publishers, Dordrecht, 2003.
- (3) Yu. Ts. Oganessian, V. K. Utyonkov, Yu. V. Lobanov, F. Sh. Abdullin, A. N. Polyakov, I. V. Shirokovsky, Yu. S. Tsyganov, G. G. Gulbekian, S. L. Bogomolov, B. N. Gikal, A. N. Mezentsev, S. Iliev, V. G. Subbotin, A. M. Sukhov, A. A. Voinov, G. V. Buklanov, K. Subotic, V. I. Zagrebaev, M. G. Itkis, J. B. Patin, K. J. Moody, J. F. Wild, M. A. Stoyer, N. J. Stoyer, D. A. Shaughnessy, J. M. Kenneally, and R. W. Loughheed, *Nucl. Phys. A* **734**, 109 (2004).
- (4) Yu. Ts. Oganessian, V. K. Utyonkov, Yu. V. Lobanov, F. Sh. Abdullin, A. N. Polyakov, I. V. Shirokovsky, Yu. S. Tsyganov, G. G. Gulbekian, S. L. Bogomolov, A. N. Mezentsev, S. Iliev, V. G. Subbotin, A. M. Sukhov, A. A. Voinov, G. V. Buklanov, K. Subotic, V. I. Zagrebaev, M. G. Itkis, J. B. Patin, K. J. Moody, J. F. Wild, M. A. Stoyer, N. J. Stoyer, D. A. Shaughnessy, J. M. Kenneally, and R. W. Loughheed, *Phys. Rev. C* **69**, 021601 (2004).
- (5) K. Morita, K. Morimoto, D. Kaji, T. Akiyama, S. Goto, H. Haba, E. Ideguchi, R. Kanungo, K. Katori, H. Koura, H. Kudo, T. Ohnishi, A. Ozawa, T. Suda, K. Sueki, H. S. Xu, T. Yamaguchi, A. Yoneda, A. Yoshida, and Y. L. Zhao, *J. Phys. Soc. Jpn.* **73**, 2593 (2004).
- (6) P. J. Karol, H. Nakahara, B. W. Petley, and E. Vogt, *Pure Appl. Chem.* **75**, 1601 (2003).
- (7) B. Fricke and W. Greiner, *Phys. Lett.* **30B**, 317 (1969).
- (8) P. Pyykkö, *Chem. Rev.* **88**, 563 (1988).
- (9) V. Pershina, *Chem. Rev.* **96**, 1977 (1996).
- (10) P. Schwerdtfeger and M. Seth, *Encyclopedia of Computational Chemistry*, Vol. 4, eds. P. von R. Schleyer et al., Wiley, New York, 1998, p. 2480.
- (11) J. V. Kratz, *Chemistry of Transactinides*. In: *Handbook of Nuclear Chemistry*, Vol. 2, *Elements and Isotopes*, eds. A. Vértes, S. Nagy, Z. Klencsár, Kluwer Academic Publishers, Dordrecht, 2003, p. 323.
- (12) M. Schädel, *J. Nucl. Radiochem. Sci.* **3**, 113 (2002); M.

- Schädel, *Acta Phys. Polonica B* **34**, 1701 (2003).
- (13) H. Haba, K. Tsukada, M. Asai, I. Nishinaka, M. Sakama, S. Goto, M. Hirata, S. Ichikawa, Y. Nagame, T. Kaneko, H. Kudo, A. Toyoshima, Y. Shoji, A. Yokoyama, A. Shinohara, Y. Oura, K. Sueki, H. Nakahara, M. Schädel, J. V. Kratz, A. Türler, and H. W. Gäggeler, *Radiochim. Acta* **89**, 733 (2001).
- (14) Y. Nagame, M. Asai, H. Haba, S. Goto, K. Tsukada, I. Nishinaka, K. Nishio, S. Ichikawa, A. Toyoshima, K. Akiyama, H. Nakahara, M. Sakama, M. Schädel, J. V. Kratz, H. W. Gäggeler, and A. Türler, *J. Nucl. Radiochem. Sci.* **3**, 85 (2002).
- (15) H. Haba, K. Tsukada, M. Asai, S. Goto, A. Toyoshima, I. Nishinaka, K. Akiyama, M. Hirata, S. Ichikawa, Y. Nagame, Y. Shoji, M. Shigekawa, T. Koike, M. Iwasaki, A. Shinohara, T. Kaneko, T. Maruyama, S. Ono, H. Kudo, Y. Oura, K. Sueki, H. Nakahara, M. Sakama, A. Yokoyama, J. V. Kratz, M. Schädel, and W. Bröchle, *J. Nucl. Radiochem. Sci.* **3**, 143 (2002).
- (16) H. Haba, K. Tsukada, M. Asai, A. Toyoshima, K. Akiyama, I. Nishinaka, M. Hirata, T. Yaita, S. Ichikawa, Y. Nagame, K. Yasuda, Y. Miyamoto, T. Kaneko, S. Goto, S. Ono, T. Hirai, H. Kudo, M. Shigekawa, A. Shinohara, Y. Oura, H. Nakahara, K. Sueki, H. Kikunaga, N. Kinoshita, N. Tsuruga, A. Yokoyama, M. Sakama, S. Enomoto, M. Schädel, W. Bröchle, and J. V. Kratz, *J. Am. Chem. Soc.* **126**, 5219 (2004).
- (17) R. B. Firestone and V. S. Shirley, *Table of Isotopes*, 8th ed. John Wiley and Sons, New York (1996).
- (18) A. Ghiorso, M. Nurmia, K. Eskola, and P. Eskola, *Phys. Lett.* **32B**, 95 (1970).
- (19) R. J. Silva, P. F. Dittner, M. L. Mallory, O. L. Keller, K. Eskola, P. Eskola, M. Nurmia, and A. Ghiorso, *Nucl. Phys.* **A216**, 97 (1973).
- (20) J. V. Kratz, *Pure Appl. Chem.* **75**, 103 (2003).
- (21) R. Guillaumont, J. P. Adloff, and A. Peneloux, *Radiochim. Acta* **46**, 169 (1989).
- (22) R. Guillaumont, J. P. Adloff, A. Peneloux, and P. Delamoye, *Radiochim. Acta* **54**, 1 (1991).
- (23) R. J. Borg and G. J. Dienes, *J. Inorg. Nucl. Chem.* **43**, 1129 (1981).
- (24) Y. Nagame, K. Tsukada, M. Asai, A. Toyoshima, K. Akiyama, Y. Ishii, T. Kaneko-Sato, M. Hirata, I. Nishinaka, S. Ichikawa, H. Haba, S. Enomoto, K. Matsuo, D. Saika, Y. Kitamoto, H. Hasegawa, Y. Tani, W. Sato, A. Shinohara, M. Ito, J. Saito, S. Goto, H. Kudo, H. Kikunaga, N. Kinoshita, A. Yokoyama, K. Sueki, Y. Oura, H. Nakahara, M. Sakama, M. Schädel, W. Bröchle, and J. V. Kratz, *Radiochim. Acta* (in press).
- (25) M. Schädel, W. Bröchle, E. Jäger, E. Schimpf, J. V. Kratz, U. W. Scherer, and H. P. Zimmermann, *Radiochim. Acta* **48**, 171 (1989).
- (26) Y. Nagame, H. Haba, K. Tsukada, M. Asai, K. Akiyama, M. Hirata, I. Nishinaka, S. Ichikawa, H. Nakahara, S. Goto, T. Kaneko, H. Kudo, A. Toyoshima, A. Shinohara, M. Schädel, J. V. Kratz, H. W. Gäggeler, and A. Türler, *Czech. J. Phys.* **53**, A299 (2003).
- (27) A. Toyoshima, K. Tsukada, H. Haba, M. Asai, S. Goto, K. Akiyama, I. Nishinaka, S. Ichikawa, Y. Nagame, and A. Shinohara, *J. Radioanal. Nucl. Chem.* **255**, 485 (2003).
- (28) E. K. Hulet, R. W. Loughheed, J. F. Wild, J. H. Landrum, J. M. Nitschke, and A. Ghiorso, *J. Inorg. Nucl. Chem.* **42**, 79 (1980).
- (29) V. Pershina, D. Trubert, C. Le Naour, and J. V. Kratz, *Radiochim. Acta* **90**, 869 (2002).
- (30) Y. Nagame, H. Haba, K. Tsukada, M. Asai, A. Toyoshima, S. Goto, K. Akiyama, T. Kaneko, M. Sakama, M. Hirata, T. Yaita, I. Nishinaka, S. Ichikawa, and H. Nakahara, *Nucl. Phys.* **A734**, 124 (2004).
- (31) H. Haba, K. Akiyama, K. Tsukada, M. Asai, A. Toyoshima, T. Yaita, M. Hirata, K. Sueki, and Y. Nagame, In: *Advances in Nuclear and Radiochemistry*, eds. S. M. Qaim, H. H. Coenen, Forschungszentrum Jülich GmbH, Jülich, 2004, p. 150; H. Haba, K. Akiyama, K. Tsukada, M. Asai, A. Toyoshima, T. Yaita, M. Hirata, K. Sueki, and Y. Nagame, to be submitted.
- (32) E. H. Huffman, G. M. Iddings, and R. C. Lilly, *J. Am. Chem. Soc.* **73**, 4474 (1951).
- (33) A. Toyoshima, H. Haba, K. Tsukada, M. Asai, K. Akiyama, I. Nishinaka, Y. Nagame, D. Saika, K. Matsuo, W. Sato, A. Shinohara, H. Ishizu, M. Ito, J. Saito, S. Goto, H. Kudo, H. Kikunaga, N. Kinoshita, C. Kato, A. Yokoyama, and K. Sueki, *J. Nucl. Radiochem. Sci.* **5**, 45 (2004).
- (34) C. D. Kacher, K. E. Gregorich, D. M. Lee, Y. Watanabe, B. Kadkodayan, B. Wierczinski, M. R. Lane, E. R. Sylwester, D. A. Keeney, M. Hendricks, and D. C. Hoffman, *Radiochim. Acta* **75**, 135 (1996).
- (35) D. Schumann, H. Nitsche, St. Taut, D. T. Jost, H. W. Gäggeler, A. B. Yakushev, G. V. Buklanov, V. P. Domanov, D. T. Lien, B. Kubica, R. Misiak, and Z. Szełgowski, *J. Alloys Comp.* **271-273**, 307 (1998).
- (36) E. Strub, J. V. Kratz, A. Kronenberg, A. Nähler, P. Thörle, S. Zauner, W. Bröchle, E. Jäger, M. Schädel, B. Schausten, E. Schimpf, Li Zhogwei, U. Kirbach, D. Schumann, D. Jost, A. Türler, M. Asai, Y. Nagame, M. Sakama, K. Tsukada, H. W. Gäggeler, and J. P. Glatz, *Radiochim. Acta* **88**, 265 (2000).
- (37) A. Kronenberg, K. Eberhard, J. V. Kratz, P. K. Mohapatra, A. Nähler, P. Thörle, W. Bröchle, M. Schädel, and A. Türler, *Radiochim. Acta* **92**, 379 (2004).
- (38) P. M. Plaisance and R. Guillaumont, *Radiochim. Acta* **12**, 32 (1969).
- (39) J. I. Kim, H. Lagally, and H.-J. Born, *Anal. Chim. Acta* **64**, 29 (1973).
- (40) J. Korkisch, *Handbook of Ion Exchange Resins: Their Application to Inorganic and Analytical Chemistry*, CRC Press, Boca Raton, FL, 1989.
- (41) A. Toyoshima, Ph. D thesis, Osaka University, 2004.
- (42) M. Hirata, private communication.
- (43) R. G. Pearson, *J. Am. Chem. Soc.* **85**, 3533 (1963).
- (44) E. Johnson and B. Fricke, *J. Phys. Chem.* **95**, 7082 (1991).
- (45) K. Tsukada, H. Haba, M. Asai, A. Toyoshima, K. Akiyama, I. Nishinaka, M. Hirata, K. Hashimoto, S. Ichikawa, Y. Nagame, K. Yasuda, Y. Miyamoto, Y. Tani, H. Hasegawa, W. Sato, A. Shinohara, S. Goto, M. Ito, J. Saito, H. Ishizu, H. Kudo, Y. Oura, H. Nakahara, K. Sueki, N. Kinoshita, H. Kikunaga, and A. Yokoyama, In: *Advances in Nuclear and Radiochemistry*, eds. S. M. Qaim, H. H. Coenen, Forschungszentrum Jülich GmbH, Jülich, 2004, p. 155.